IOP Conference Series: Materials
Science and Engineering

PAPER • **OPEN ACCESS**

Flexural performance of the wood core composite T section beams

To cite this article: Lei Wu *et al* 2019 *IOP Conf. Ser.: Mater. Sci. Eng.* **493** 012011

IOP Conf. Series: Materials Science and Engineering **493** (2019) 012011 doi:10.1088/1757-899X/493/1/012011

Flexural performance of the wood core composite T section beams

Lei Wu [a], **Yujun Qi** [b, *], **Weiqing Liu** [c]

College of Civil Engineering, Nanjing Tech University, Nanjing 211816, China;

[a] 1442408854@qq.com; [*, b] Corresponding author e-mail qiyujuncn@yeah.net;
[c] wqliu@njtech.edu.cn

Abstract. A new type of T section beam is proposed in this paper, which is mainly composed of Fiber reinforced polymers (FRP) shell and light wood core. The wood core composite T section beams has the following advantages:the integration of the vacuum infusion technology, can avoid the problem of interface slip of steel-concrete beams in the actual process, and between with the traditional composite beam interface with shear stud connections, few construction procedures, relatively simple, but also further improving the interface properties of T section beams. Through four point bending test, the mechanical properties, failure mode, flexural capacity, stiffness and ductility of T section beam with wood core composite were obtained. The test results show that the T-400-60 specimens compared to the specimens of T-400-40 and T-400-20 specimens, the bearing capacity is increased by 34% and 46%, while the stiffness is increased by 40% and 49% respectively, indicating the flange height type of The wood core composite T section beams on the bearing capacity and stiffness of the great influence.

Keywords: Fiber reinforced polymer (FRP); Paulownia wood; T section beams; Vacuum infusion; Bearing capacity.

1. Introduction

Fiber reinforced polymer (FRP) have the advantages of light weight, high strength, high durability and strong bearing capacity. Therefore, in recent years, this material has been applied to many structural and unstructured fields. GFRP material plays an important role in bridge engineering and building engineering[1-3]. Construction projects are mainly about the non load-bearing structural components, such as the walls and roofs of temporary buildings[4].

At present, the common T section beams in the construction industry include steel-concrete mixed T section beams.many scholars at home and abroad have made a lot of scientific research on the mechanical characteristics of this kind of steel-concrete composite structure[5-6],this new T section beams have a relatively small weight, good bearing capacity and ductility, favorable to structure earthquake etc.. At the same time, there are some shortcomings, for example, in coastal and marine engineering, how to improve the corrosion resistance of steel is the key problem that needs to be solved[7].The wooden beams and concrete combine to form wood-concrete T section beams, this kind of T section beams make the two materials do their best, collaborative work and give full play to their material properties. Beside, there is no problem of corrosion of steel. Hu Xiamin[8] Studied on the flexural behavior of wood-concrete T section beams subjected to static load.The deformation development process and failure form of wood-concrete T section beams are investigated and draw the conclusion: with the decreasing degree of shear connection, T section beams deformation and the interface slip increases, while the elastic flexural bearing capacity decreases the flexural stress and limit, but it is not proportional to the shear connection degree and the interface slip is more prominent. Later, foreign scholars Cassity and zhou[9-12] began to study GFRP-steel T section beams, the T section beam can give full play to the characteristics of the steel and GFRP composite lightweight, corrosion resistance and other advantages, they put forward three different forms of interface connection, mechanical connections, adhesive connections and mixed connections, each have advantages and disadvantages, but the slip the problem remains to be solved between different materials.

According to the actual needs of the project, a new type of wood core composite T section beam is designed, which is made up of GFRP composite material and paulownia wood core material, and then is made by vacuum induction technology. The bending resistance test of this wood core composite T section beam is carried out, and the load displacement relation, failure mode and ultimate bearing capacity are obtained. In addition, there is no significant slip phenomenon between the sections. At the same time, when the load reaches the maximum value, there is no sudden sudden drop, which has better ductility characteristics. Finally, the first order shear deformation theory[13] is used to predict the deformation of the T section beam under the elastic state. In general, the results of the theory are in good agreement with the experimental results, which can meet the application of the engineering.

2. Test situation

2.1. The specimen design

In this experiment, 3 kinds of wood core composite T section beams are designed. The following expressions are as follows: T represents T section beam, 400 represents flange width, 60 indicates flange height, and the specific specimen information is shown in Table 1. In the case of T-400-60 specimen, the internal flange was composed of four paulownia wood core material with 98*54*2000mm, the web was composed of two paulownia wood core material with 58*54*2000mm, and covered with a layer of GFRP material in Paulownia wood, in the end the combination of T section beams and the formation of integration by vacuum infusion.

Table 1. Specimen parameters

type	L (mm)	bf' (mm)	hf' (mm)
T-400-60	2000	400	60
T-400-40	2000	400	40
T-400-20	2000	400	20

2.2. Material properties

The basic mechanical properties of the surface layer GFRP and paulownia wood core are shown in Table 2

2.3. Measurement scheme and setup

The four point bending loading method is used in this experiment, which is illustrated in Figure1. The T section beams length of 2000mm, is placed in a fixed hinge bearing, the other end is arranged in a sliding hinge support, and the span of 1800mm, and in order to measure real

Table 2. Mechanical properties of GFRP and Paulownia wood

Type	Compressive strength/MPa	Tensile strength/MPa	Elastic modulus/GPa	Shear modulus/GPa
GFRP	168.21	210	22.0	18.5
Paulownia wood	21.50	49.2	4.3	0.464

Situation, the test between the loading head and the loading head set size of 100*100*400mm steel pad, at the same time, the deformation of wood core composite T section beams was measured by displacement meter and 5AA strain gauge, five displacement meter is arranged in the middle vertical position of loading point at the bottom and T section beam. At the same time, the strain gauge lay out wood core composite beam at the top and bottom, the strain measuring point arrangement as shown in figure 2. At the early stage of loading, the load of T-400-60 specimen, T-400-40 specimen and T-400-20 specimen was 5KN, 5KN and 3KN respectively. When the test beams was damaged and the load is significantly reduced, the load was stopped when the deflection is loaded to 1/15, which is greater than the span of the beam, as the ultimate failure mode.

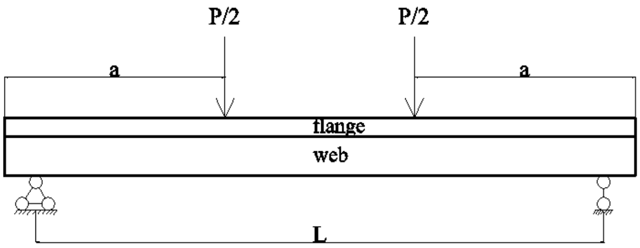

Fig.1 Test setup

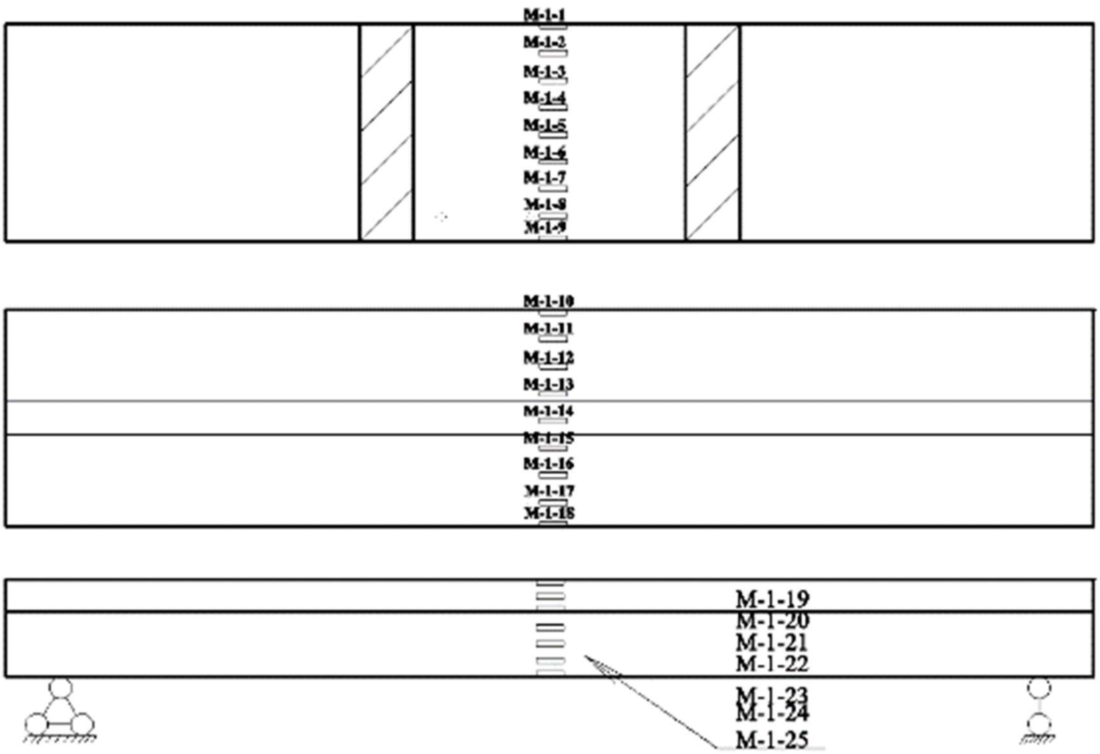

Fig.2 The Points layout

3. Failure mode

3.1. T-400-60 specimen

When the load was 60KN, the sound of crackle began to appear, and longitudinal cracks appeared at the junction of paulownia wood core on both sides. As shown in Fig.3a. with the increased of load, when the load was 85KN, the crack extended to the side of the support, as shown in Fig.3b, 3c. Continued to increase the load, cracks continued to expand, when the load was loaded into the 105KN, the deflection was 40.87mm, about 1/44 net cross beam, then hearded a huge noise, the load decreased to 102KN, then continued to increase the load, the deflection continued to increase, the horizontal cracks below the load point began to appear as shown in Fig.3d. then continued loading, cracks continue to expanded, when the load increased to the maximum value of 108.9KN, the thickness of crack entirely through the flange, the corresponding deflection was 55.27mm, about 1/33 of the beam span, and the load decreased to 107kN, indicating that The shear failure at the junction of the flange and the web made the internal force of the core redistributed. When loading continued, cracks appeared at the flange web connections at the front and rear sides of the T section beam, but the inner core material did not appear obvious slip phenomenon. as the load increased, the crack continued to extend to the support, as shown in Fig.3e. With the increase of load, the deflection started smoothly, and when the load was 92KN, the deflection was 115mm, about 1/16 of the beam span, The deformation of the component was too large at this time, as the ultimate failure form, as shown in Fig.3f. the main failure mode was yielding surface layer, resulting in a decline in bearing capacity.

Fig.3a

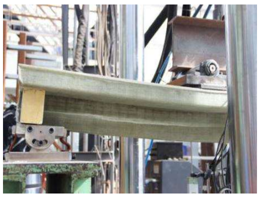

Fig.3b

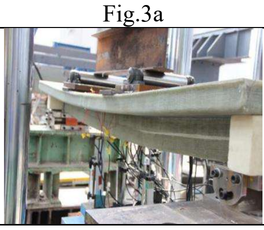

Fig.3c

Fig.3d

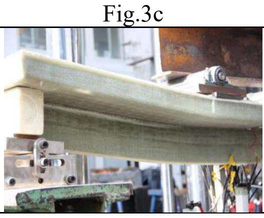

Fig.3e

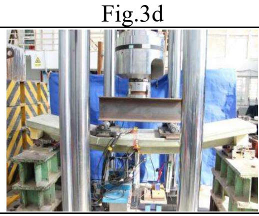

Fig.3f

Fig.3 Failure mode of T-400-60 specimen

3.2. T-400-40 specimen

Compared with the T-400-60 specimen, the damage of T-400-40 specimen was earlier. when loaded to 48KN, flange and web junction also appeared crack, as shown in Fig.4a. and began to extend to the seat, when the load was 75KN, the huge noise was heard , and the load decreased to 70.2KN, while the side loading bottom beam flange the transverse cracks began to appear, as shown in Fig.4b, Continue loading, the cracks continue to expand, when load was maximum load 81.4KN, the deflection was about 59.32mm, about 1/30 of the span, and heard a huge noise, load decreased to 78.5KN, the transverse cracks quickly extended to the flange thickness direction, entirely through the flange as shown in Fig.4c. Then when the load was 71.3KN, the deflection was 98.3mm, about 1/18 of the span, deformation was too large, as the final failure form. As shown in Fig.4d. the test showed that the main failure mode of the specimen was shear failure along the surface layer below the loading beam, and there was no larger brittle failure.

	
Fig.4a	Fig.4b
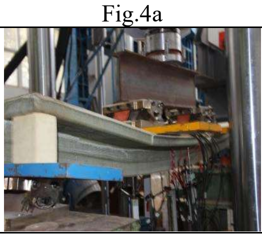	
Fig.4c	Fig.4d

Fig.4 Failure mode of T-400-40 specimen

3.3. T-400-40 specimen

Compared with two former groups of specimens, the failure mode of T-400-20 specimen was more obvious, when the load was 36kN, there was fiber cracks as shown in Fig.5a, when the load increased to 52KN, a huge noise was heard , while the load decreased to 46.3KN, mainly due to the huge decline in the load in the elastic stage is flange a thin, elastic flexural rigidity, extrusion fracture by internal core material, the load declined slightly, while one side of the load beam bottom flange crack began to appear, as shown in Fig.5b, the T section beams still continue to bear the load, the crack load below the flange along the transverse beam at the same time, the other side was extended below the load beam cracks began to appear, when loaded to the maximum load 74.6KN, the deflection was about 71.8mm, about 1/25 of the span, and heard the noise load dropped to 7 0.5KN, at this time, the transverse crack rapidly expanded to the direction of the flange thickness, which running through the flange, as shown in the Fig.5c, When the load was 63.8KN, the deflection was 90.3mm, about 1/20 of the span, it was the final failure form. As shown in Fig.5d, The test shows that the ultimate failure mode of the three kinds of components was similar, mainly the shear failure of the layer under the loading beam, so that the deformation of the component was too large.

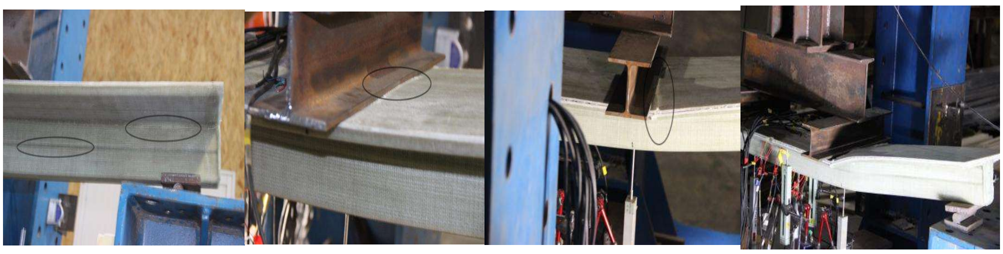

(a) (b) (c) (d)

Fig.5 Failure mode of T-400-20 specimen

4. Results and discussion

4.1. Load displacement curve

The load displacement curves of three kinds of T section beams with different flange height are shown in Fig.6, three kinds of T section beams under four point bending load, before the maximum elastic stage, the load deflection curve showed a linear change, that was elastic stress stage; then the jitter rose and all began to fall down, mainly due to the shear failure at the junction of the flange and the web made the internal force of the core redistributed, continued to be the maximum value, after peak load, three kinds of T section beams had good ductility, load slow down a bit, and no significant decline, owned good ductility.

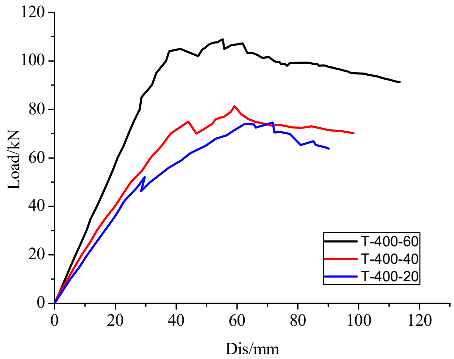

Fig.6 Comparison of load displacement curves

4.2. Strength and stiffness

The test results of all T section beams include ultimate flexural strength P_u, elastic flexural strength P_y and the corresponding deflection f_y of the mid span in the elastic stage and elastic stiffness k_e are listed in Table 3. In this paper, k_e is calculated from the initial line elastic part of the load deflection curve of each specimen.

Table 3. Mechanical parameters of specimens

Specimens	P_u *(kN)*	P_y *(kN)*	f_y *(mm)*	K_e (kN/mm)
T-400-60	108.9	80	23.97	2.67
T-400-40	81.4	55	28.67	1.91
T-400-20	74.6	45	25.04	1.79

For the T-400-60 specimen, the ultimate bending strength Pu is 33% and 46%, compared with the T-400-40 specimen and the T-400-20 specimen respectively. Meanwhile, the elastic stiffness ke is about 1.39, 1.49 times of the T-400-40 specimen and the T-400-20 specimen. The bearing capacity of different flange is the main reason for the different height of specimen, at the same time, little difference in bending stiffness between the T-400-40 specimen and the

T-400-20 specimen, when the load is less than 40KN, the flange height is not main reason. It can be found that with the change of flange height, the bearing capacity and actual stiffness have changed, and the higher the flange height, the higher the actual bearing capacity, the greater the stiffness.

5. Theoretical analysis

According to the classical Euler Bernoulli beam theory, considering the flexural and shear deformation of elastic stage, the theoretical formula is used to calculate the results and compared with the experimental values, the overall results are similar.The schematic diagram of the specific model analysis is shown in Fig.7. The first order shear deformation theory can be used to solve the deflection problem, and the mid span deflection can be calculated according to the formula (1).

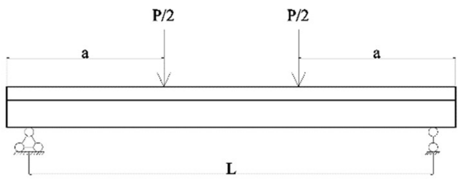

Fig.7 The form of force about the T Section beams

$$\Delta = w_1 + w_2 = \frac{P \cdot \mathrm{a} \cdot \left(3\mathrm{l}^2 - 4a^2\right)}{48EI} + \frac{P\mathrm{a}}{2GA} \tag{1}$$

Where P is the load, L is the span, a is the distance from the end of the loading point, GA, EI are the elastic flexural stiffness and elastic shear stiffness.

5.1. Elastic flexural rigidity

According to the plane cross-section assumption, the bending stiffness is equal to the sum of the bending stiffness of the surface layer, the web and the core, and the theoretical analysis model is shown in Fig.8, The overall EI of all kinds of T section beams specimens are similar, and take the T-400-60 specimen as an example.

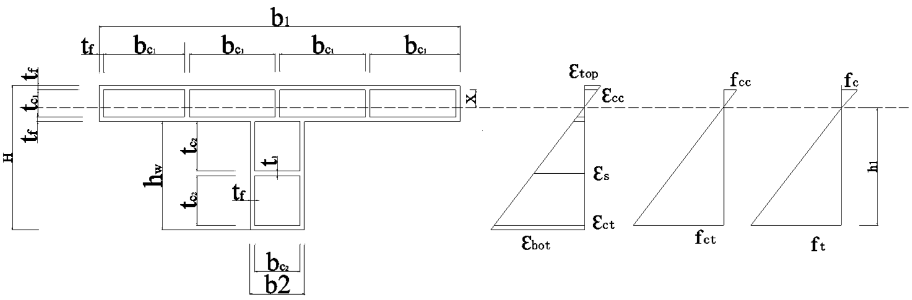

Fig.8 Sectional measure of T section beams

$$\begin{aligned} EI &= 4(EI)_{c1} + 2(EI)_{f1} + 2(EI)_{w1} \\ &\quad + 2(EI)_{c2} + (EI)_{f2} + 2(EI)_{w2} \end{aligned} \tag{2}$$

According to the theoretical of sandwich plate:

$$\begin{aligned}EI = & E_C\left(\frac{b_{c1}\cdot t_{c1}^3}{3}+\frac{b_{c2}\cdot t_{c2}^3}{6}\right)+2t_f\cdot t_{c1}\cdot\left(x-\frac{t_{c1}}{2}\right)^2 \\ & +4b_{c1}\cdot t_{c1}\cdot\left(x-\frac{t_{c1}}{2}\right)^2+b_1\cdot t_f\left[\left(x+\frac{t_f}{2}\right)^2+\left(\frac{t_f}{2}+t_{c1}-\mathrm{x}\right)^2\right] \\ & +b_{c2}\cdot t_{c2}\cdot\left[\left(\frac{t_{c2}}{2}+t_f+t_{c1}-x\right)^2+\left(h_w-\frac{t_{c2}}{2}+\mathrm{t}_{c1}-x\right)^2\right] \\ & +b_{c2}\cdot t_f\left(h_{\mathrm{w}}+\frac{t_f}{2}+t_{c1}-x\right)^2+2t_f\cdot h_w\left(\frac{h_w}{2}+t_f+t_{c1}-x\right)^2 \\ & +E_{gf}\left(\frac{b_1\cdot t_f^3}{6}+\frac{t_f\cdot t_{c1}^3}{6}+\frac{b_{c2}\cdot t_f^3}{12}+\frac{t_f\cdot h_w^3}{6}\right)\end{aligned} \tag{3}$$

x is the distance between the top of the core and the neutral axis. As shown in Fig.8, the compressive stress C is equal to the tensile stress T.

$$\sum X=0\ T=C$$

$$C=C_f+C_w+C_c \qquad C_f=b_1 t_f E_f\cdot\frac{\varepsilon_{cc}+\varepsilon_{top}}{2}$$

$$C_w=2x\cdot t_f\cdot E_f\cdot\varepsilon_{cc} \qquad C_c=4f_{cc}\frac{x\cdot b_{c1}}{2}$$

$$T=T_{uf}+T_{uw}+T_{uc}+T_{df}+T_{dw}+T_{dc}$$

$$T_{uf}=b_1 t_f E_f\cdot\frac{\varepsilon_{ct}+\varepsilon_{bot}}{2}$$

$$T_{uw}=2(t_{c1}-x)\cdot t_f\cdot E_f\cdot\varepsilon_{ct}$$

$$T_{uc}=4f_{ct}\frac{t_{c1}-x}{h_1}\cdot\frac{t_{c1}-x}{2}\cdot b_{c2}$$

$$T_{df}=b_2 t_f E_f\cdot\frac{\varepsilon_{ct}+\varepsilon_{bot}}{2}$$

$$T_{dw}=2h_w\cdot t_f\cdot E_f\cdot\varepsilon_{ct}$$

Then:

$$\varepsilon_{bot}=\frac{f_{ct}}{E_f} \qquad \varepsilon_{ct}=\frac{h_w-t_f}{h_w}\cdot\varepsilon_{bot}$$

$$\varepsilon_{top}=\frac{f_{cc}}{E_f} \qquad \varepsilon_{cc}=\frac{x}{x+t_f}\cdot\varepsilon_{top}$$

And the specific mechanical properties and materials size, including *bc1, b1, bc2, b2* are the width of the upper single core, the total width of the upper part of the specimen, the width of the lower single core, and the total width of the lower part of the specimen. *tf* is the surface thickness, *tw* is the web thickness, and *tc1,tc2* are the height of the upper core and the lower core, respectively. *hw,H* are the height of the bottom web and the height of the whole T section beam.The specific dimensions are shown in Table 1 and table 2, and the x can be finally obtained. *EI* can be obtained by replacing the x into the formula (3).

5.2. Shear stiffness

The shear stiffness of wood core composite T section beams is composed of paulownia wood core, GFRP web and GFRP surface shear stiffness.The specific schematic diagram is shown in Fig 8. Ggf is the shear modulus of the web, and the GA of all kinds of T section beams are similar, and the specimen T-400-60 is taken as an example.

$$\begin{aligned} GA &= 4(GA)_{c1} + 2(GA)_{f1} + 2(GA)_{w1} + 2(GA)_{c2} \\ &+ (GA)_{f2} + 2(GA)_{w2} \end{aligned} \tag{4}$$

According to the theoretical of sandwich plate:

$$\begin{aligned} GA &= G_{gf} \cdot \left(2b_1 \cdot t_f + 2\mathrm{t}_f \cdot t_{c1} + b_{c2} \cdot \mathrm{t}_f + 2t_f \cdot \mathrm{h}_w\right) \\ &+ G_c \cdot \left(4b_{c1} \cdot t_{c1} + 2b_{c2} \cdot t_{c2}\right) \end{aligned} \tag{5}$$

Taking EI and GA into the above formula (1), a theoretical solution of the load displacement curve of a T section beam with three different flange height can be obtained (shown in Fig.9). Among them, Ex and Th respectively indicate the experimental values and theoretical values. As can be seen from Fig.9, the theoretical value is in good agreement with the experimental data. The main reason for the experimental value is less than the theoretical value is that the actual bearing capacity has slightly decreased after the failure of the surface layer, and the overall error is not large enough to meet the practical application of the project.

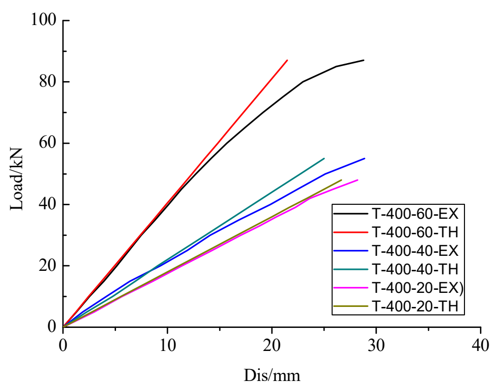

Fig.9 Theoretical and experimental values of load-displacement curve

6. Conclusion

(1) The mainly failure mode of the wood core composite T section beams is the compression failure of the flange surface layer.

(2) For the T-400-60 specimen, the bearing capacity is increased by 33% and 46%, when comparing with the T-400-40 specimen and the T-400-20 specimen. at the same time, the elastic stiffness is1.39 times and 1.49 times that two specimens, which indicates the height of the flange has a great influence on the bearing capacity and stiffness.

(3) The bearing capacity of the wood core composite T section beams reache the maximum value, and there is no large load drop. It shows that the T beam has good ductility, which is very good for engineering application.

(4) The larger the load is, the larger of the difference between the theoretical value and the experimental value is mainly due to the increase of cracks at the interface between flange and web, when

going into the plastic stage. The overall elastic stage error is relatively small, which has larger scientific research value.

References

[1] K Coogler, KA Harries, B Wan, DC Rizos, MF Petrou. Critical Evaluation of Strain Measurements in Glass Fiber-Reinforced Polymer Bridge Decks[J]. Journal of Bridge Engineering, 2005, 10 (6) :704-712.
[2] KJ Hong, SW Lee. Experiencing More GFRP Composite Bridge Decks for Vehicular and Pedestrian Bridges[J]. Iabse Congress Report, 2008.
[3] Lee SW, Hong KJ. Constructing bridges with glass-fiber reinforced composite decks. In: Proceedings of 4th international structural engineering and construction. Melbourne (Australia): RMIT University. 2007.
[4] Wuhan Architectural Material Industry Institute of glass and steel teaching and research department. The application of FRP in the building. China Architecture Industry Press, 1980.
[5] Nie Jianguo, Li Yong, Yu Zhiwu. Steel-concrete beams stiffness[J]. Journal of Tsinghua University Natural Science Edition, 1998, 38(10): 38-41.
[6] Nie Jianguo, Wang Hongquan, Tan Ying. Experimental study of steel high strength concrete composite beams[J]. Journal of architectural structure, 2004, 25(1): 58-62.
[7] Xia Wenmin, Liu Xuemei. Research status and Prospect of steel-concrete composite beam[J]. Journal of architectural structure of Central South University. 2009.
[8] Hu Xiaming, Li Qiao, Peng Hongyi. Wood-concrete composite beam static research[J]. 2007, 39 (3): 24-36.
[9] Cassity P, Richard D, Gillespie J. Composite acting FRP deck and girder systerm[J]. Internatioal Structural Engineering, 2002, 12(2):71-75.
[10] Zhou A X, Thomas K. Joining techniques for fiber reinforced polymer composite bridge deck systerm[J]. Composite Structures, 2005, 69:336-345.
[11] Salim HA, Davalos JF. FRP composite short-span bridges: Analysis, design and testing[J]. Journal of advanced materials, 1999,31(1):18-16.
[12] Qiao P, Davalos J F, Brown B. A systematic approach for analysis and design of single-span FRP deck/stringer bridges[J]. Composites Part B, 2000,31(6-7):593-610.
[13] Carlsson L A, Kardomateas G A. Structural and failure mechanics of sandwich composites, Springer, New York. (2011).